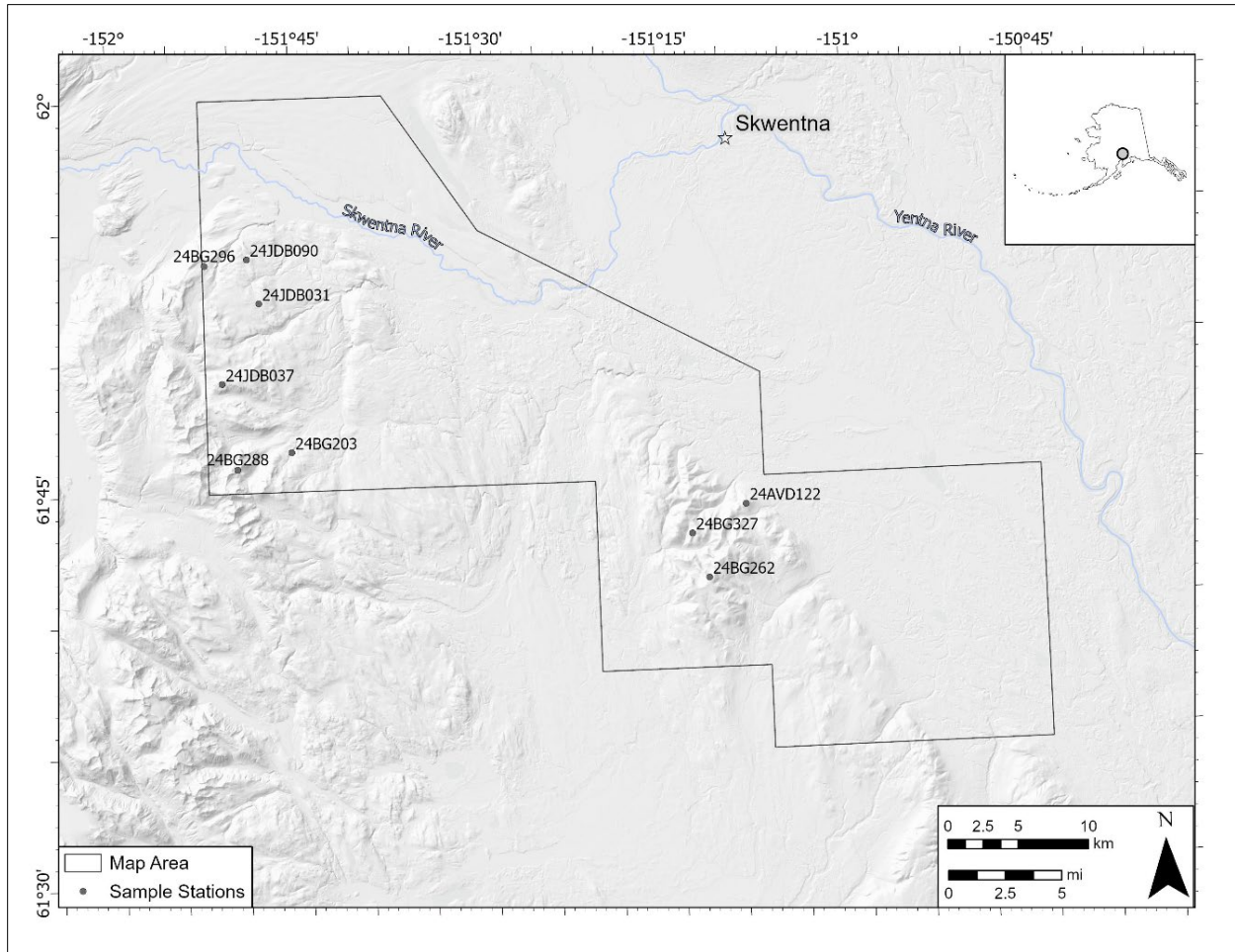


ZIRCON U-PB GEOCHRONOLOGY FOR BEDROCK SAMPLES FROM THE WEST SUSITNA STATEMAP PROJECT, SOUTHCENTRAL ALASKA

Robert J. Gillis, Sandra L. Walser, John D. Bernt, and Paul B. O'Sullivan

Raw Data File 2026-8



Location map of samples selected for uranium-lead geochronology in the map area.

Publications in the DGGs RDF series provide elevation data, field observations, or analytical results. The data have been reviewed for clarity and consistency but have not undergone technical peer review.

2026
STATE OF ALASKA
DEPARTMENT OF NATURAL RESOURCES
DIVISION OF GEOLOGICAL & GEOPHYSICAL SURVEYS



STATE OF ALASKA

Mike Dunleavy, Governor

DEPARTMENT OF NATURAL RESOURCES

John Crowther, Commissioner-Designee

DIVISION OF GEOLOGICAL & GEOPHYSICAL SURVEYS

Erin Campbell, State Geologist & Director

Publications produced by the Division of Geological & Geophysical Surveys are available to download from the DGGS website (dgg.alaska.gov). Publications on hard-copy or digital media can be examined or purchased in the Fairbanks office:

Alaska Division of Geological & Geophysical Surveys (DGGS)

3354 College Road | Fairbanks, Alaska 99709-3707

Phone: 907.451.5010 | Fax 907.451.5050

dggspubs@alaska.gov | dgg.alaska.gov

DGGS publications are also available at:

Alaska State Library, Historical
Collections & Talking Book Center
395 Whittier Street
Juneau, Alaska 99801

Alaska Resource Library and
Information Services (ARLIS)
3150 C Street, Suite 100
Anchorage, Alaska 99503

Suggested citation:

Gillis, R.J., Walser, S.L., Bernt, J.D., and O'Sullivan, P.B., 2026, Zircon U-Pb geochronology for bedrock samples from the West Susitna STATEMAP project, southcentral, Alaska: Alaska Division of Geological & Geophysical Surveys Raw Data File 2026-8, 9 p. <https://doi.org/10.14509/31972>



ZIRCON U-PB GEOCHRONOLOGY FOR BEDROCK SAMPLES FROM THE WEST SUSITNA STATEMAP PROJECT, SOUTHCENTRAL ALASKA

Robert J. Gillis¹, Sandra L. Walser¹, John D. Bernt^{1*}, and Paul B. O'Sullivan²

INTRODUCTION

This data release presents zircon uranium-lead (U-Pb) geochronologic data analyzed using laser ablation-inductively coupled plasma-mass spectrometry (LA-ICP-MS). The Alaska Division of Geological & Geophysical Surveys (DGGGS) staff collected ten samples for U-Pb dating during the 2024 field season as part of the West Susitna STATEMAP project. The project is a 1:50,000-scale geologic mapping initiative to characterize geology, assess geologic hazards, and investigate tectonic features within a region of increasing interest for resource development, alternative energy, and recreation. The study area lies in the West Susitna region of southcentral Alaska. It spans approximately 500 mi² across the Tyonek C-3, C-4, D-4, and D-5 quadrangles, including approximately 50 miles of the proposed West Susitna Access Corridor, which connects Anchorage to the Happy River valley on the western margin of the Susitna Basin (Alaska Industrial Development and Export Authority, 2025). Geochronological analyses were obtained to constrain the ages of mapped bedrock units and support tectonic interpretations in the map area. These data are provided as a Raw Data File under an open end-user license and are available on the DGGGS website (<https://doi.org/10.14509/31972>).

DATA PRODUCTS

- Summary data table and accompanying data dictionary listing the compiled crystallization ages and maximum depositional ages for all analyzed grains.
- Zircon grain data tables and accompanying data dictionary with the isotopic and elemental data for each analyzed zircon spot.

METHODS

Detailed descriptions of the methods followed by GeoSep Services (GSS) to produce and process the zircon U-Pb data have been previously reviewed, evaluated, and presented in Bradley and others (2009), Hults and others (2013), and Moore and others (2015).

Sample preparation

Mineral grains were initially isolated and prepared for LA-ICP-MS analysis using both standard and customized mineral separation procedures originally outlined by Donelick and others (2005). Whole rock samples were run multiple times (minimum = 3) through a Chipmunk brand jaw crusher with the minimum jaw separation set to 2-3 mm. The crushed material was sieved through 300 µm nylon mesh, and the <300 µm size fraction was washed with tap water and allowed to dry at room temperature. Zircon grains were subsequently separated from other mineral species using a combination of a centrifuge sink with lithium metatungstate (density ~2.9

¹ Alaska Division of Geological & Geophysical Surveys, 3354 College Road, Fairbanks, AK 99709

* Former DGGGS

² GeoSep Services, 1520 Pinecone Rd., Moscow, ID 83843

g/cm³), multiple steps through a Frantz magnetic separator, a density fluid sink with diiodomethane (density ~3.3 g/cm³), and hand-panning separation procedures.

Following separation, the resulting zircon grains were mounted in epoxy resin. After curing, each 1 cm² mount was manually ground to expose internal grain surfaces using 3.0 μm and 0.3 μm Al₂O₃ slurries and then polished to a glass-like finish. Subsequently, each mount was immersed in 5.5N HNO₃ for 20.0 seconds (0.5 seconds) at 21 °C (1 °C) to remove any surface common-lead contamination.

Data collection

Each grain selected for analysis, along with the planned laser-spot location, was marked while scanning the mount under transmitted light using an optical microscope at 1500–2000× magnification. Unlike the use of Cl imagery, which provides limited information related to the exposed surface of each grain, this customized approach allows for the recognition and characterization of features located below the surface of individual grains for the purpose of avoiding problematic grains with inclusions, cracks, and other internal features that might result in spurious results. This approach also allows for a detailed evaluation of: 1) each grain's morphology and color, for the purpose of targeting grains most likely to be syn-depositional (euhedral vs. rounded, clear vs. colored), and 2) high-magnification recognition of potential zoning (different stages of grain growth) within individual grains.

Laser ablation-inductively coupled plasma-mass spectrometry (LA-ICP-MS) data collection was performed at the GeoAnalytical Laboratory, Washington State University, Pullman, Washington, U.S.A. Individual zircon grains were targeted for data collection using a New Wave YP213 213 nm solid-state laser ablation system using either a 20 or 30 μm diameter laser spot size, 5 Hz laser firing rate, and ultra-high-purity He as the carrier gas. Isotopic analyses of the ablated zircon material were performed using an Agilent 7700x quadrupole mass spectrometer with high-purity Ar as the plasma gas.

Ablation pits were on the order of ~12-15 μm deep, resulting in the analysis of significant amounts of material derived from well below the grain surface. Each analysis of 32 cycles took approximately 30 seconds to complete and consisted of a 6-second integration on peaks with the laser shutter closed (for background measurements), followed by a 24-second integration with the shutter open and the laser ablating zircon material. A 20-second delay occurred between analyses. The isotopes measured included ²⁰²Hg, ²⁰⁴(Hg + Pb), ²⁰⁶Pb, ²⁰⁷Pb, ²⁰⁸Pb, ²³²Th, ²³⁵U, and ²³⁸U. Common Pb was subtracted out using the Stacey and Kramer (1975) common Pb model for Earth. Ages and common Pb ratios were determined iteratively using a preset, session-wide minimum common Pb age (the default for each session was the age of the oldest age standard, 1099 Ma FC-1).

Data modeling

Data reduction was performed off-line using software written specifically to incorporate the data reduction equations utilized by Chang and others (2006). Previous LA-ICP-MS studies of

U-Pb zircon dating used the 'intercept' method, which assumes that the isotopic ratio varies linearly with scan number due solely to linearly varying isotopic fractionation (Gerhels and others, 2008). The data modeling approach employed here was to model background-corrected signal intensities for each isotope at each scan. Background intensity for each isotope was calculated using a fitted line (for decreasing background intensity) or using the arithmetic mean (for non-decreasing background intensity) at the global minimum of selected isotopes (^{206}Pb , ^{232}Th , and ^{238}U) for the spot. Background+signal intensity for each isotope at each scan was calculated as the median of fitted (2nd-order polynomial) intensity values from a moving window (7 scans wide) that included the scan. The precision of each background-corrected signal intensity value was calculated from the precision of the background intensity value and the precision of the background+signal intensity value.

The data collected for each spot comprise a series of scans, each representing one measurement at each mass, ordered by increasing mass. The series of data scans may be divided into background and signal+background segments. Background represents data collected prior to firing the laser. Signal+background represents data collected during laser ablation of the spot.

Two zircon U-Pb age standards were used during analysis for calibration purposes. These included the 1099 ± 0.6 Ma FC zircon (FC-1 of Paces and Miller, 1993) as the primary age standard. The secondary age standard was the 61.2 ± 0.1 Ma Tardree Rhyolite zircon (Dave Chew, personal communication). At the beginning of the LA-ICP-MS session, zircon standards (TR and FC1) were analyzed until fractionation was stable and the variance in the measured $^{206}\text{Pb}/^{238}\text{U}$ and $^{207}\text{Pb}/^{206}\text{Pb}$ ratios was at or near 1 percent. In order to correct for inter-element fractionation during the session, these standards were generally reanalyzed after each 15-30 unknowns.

The fractionation factor for each data scan, corrected for accumulated α -damage, was weighted by the ^{238}U or ^{232}Th signal value for that scan; an overall weighted mean fractionation factor across all concordant data scans was used for the final age calculation. Under the operating conditions of LA-ICP-MS sessions, fractionation factors are occasionally observed to vary strongly with scan number, decreasing with increasing scan number (presumably due to increasing ablation pit depth and its effect on fractionation; for example, Paton and others, 2010). The zircon crystal lattice is widely known to accumulate α -radiation damage (for example, Zhang and others, 2009 and references therein). It is assumed that increased α -damage in a zircon leads to a decrease in the hardness of the zircon; this, in turn, leads to a faster rate of laser penetration into the zircon during ablation, leading to dependence of isotopic fractionation on the degree of zircon lattice radiation damage. Ages calculated for all zircon age standards, when those standards were treated as unknowns, were used to construct a fractionation factor correction curve (exponential form) in terms of accumulated radiation damage. The notion of a matrix-matched zircon standard and a zircon unknown has been proposed largely on the basis of trace-element chemistry (e.g., Black and others, 2004). Time and lattice damage, parameters invisible to instruments used to characterize trace element chemistry, were introduced and applied based on measured U and Th chemistries to effectively matrix-match standard and unknown zircons.

Uranium decay constants and the $^{238}\text{U}/^{235}\text{U}$ isotopic ratio reported in Steiger and Yäger (1977) were used in this study. Errors for the isotopic ratios $^{207}\text{Pb}/^{235}\text{U}_c$ ($^{235}\text{U}_c = 137.88^{238}\text{U}$), $^{206}\text{Pb}/^{238}\text{U}$, and $^{207}\text{Pb}/^{206}\text{Pb}$ at each scan included errors from the background-corrected signal values for each isotope, the fractionation factor error, and an additional relative error term required to force 95% of the FC ages to be concordant. Ages for the ratios $^{207}\text{Pb}/^{235}\text{U}_c$, $^{206}\text{Pb}/^{238}\text{U}$, and $^{207}\text{Pb}/^{206}\text{Pb}$ were calculated for each data scan and checked for concordance; concordance here was defined as overlap of all three ages at the 1σ level (the use of a 2σ level was found to skew the results to include scans with any significant common Pb). If the number of concordant data scans for a spot was greater than zero, the more precise age from the concordant-scan-weighted ratio $^{207}\text{Pb}/^{235}\text{U}_c$, $^{206}\text{Pb}/^{238}\text{U}$, or $^{207}\text{Pb}/^{206}\text{Pb}$ was chosen as the preferred age. Asymmetrical negative-direction and positive-direction age errors were calculated by subtracting and adding, respectively, the isotopic ratio errors in the appropriate age equation (Chew and Donelick, 2012).

Common lead correction

Common Pb was subtracted out using the Stacey and Kramer (1975) common Pb model for Earth. Ages and common Pb ratio were determined iteratively using a pre-set, session-wide minimum common Pb age value. The default for each session was the age of the oldest age standard (1099 Ma FC-1 and/or FC-5z).

PREFERRED AGE

The preferred age for each analysis is presented in the “ZrnUPb-Preferred Age (Sorted)” worksheet provided with each GSS data report.

Uranium decay constants and the $^{238}\text{U}/^{235}\text{U}$ isotopic ratio reported in Steiger and Yäger (1977) were used. $^{207}\text{Pb}/^{235}\text{U}_c$ ($^{235}\text{U}_c = 137.88^{238}\text{U}$), $^{206}\text{Pb}/^{238}\text{U}$, and $^{207}\text{Pb}/^{206}\text{Pb}$ ages were calculated for each data scan and checked for concordance; concordance here was defined as overlap of all three ages at the 1σ level (the use of 2σ level was found to skew the results to include scans with significant common Pb). The background-corrected isotopic sums of each isotope were calculated for all concordant scans. The precision of each isotopic ratio was calculated by using the background and signal errors for both isotopes. The fractionation factor for each data scan corrected for accumulated α -damage and was weighted by the ^{238}U or ^{232}Th signal value for that scan; an overall weighted mean fractionation factor across all concordant data scans was used for the final age calculation.

If the number of concordant data scans for a spot was greater than zero, then either the $^{206}\text{Pb}/^{238}\text{U}$ age (zircon U-Pb grain ages <1.5 Ga) or the $^{207}\text{Pb}/^{206}\text{Pb}$ age (zircon U-Pb grain ages ≥ 1.5 Ga) was chosen as the preferred age. If zero concordant data scans were observed, then the common Pb-corrected age based on isotopic sums of all acceptable scans was chosen as the preferred age. Common Pb was subtracted out using the Stacey and Kramer (1975) common Pb model for Earth. Ages and common Pb ratio were determined iteratively using a pre-set, session-wide minimum common Pb age value (see Common lead correction, above).

Preferred age precision

Errors for the isotopic ratios $^{207}\text{Pb}/^{235}\text{U}_c$ ($^{235}\text{U}_c = 137.88^{238}\text{U}$), $^{206}\text{Pb}/^{238}\text{U}$, and $^{207}\text{Pb}/^{206}\text{Pb}$ at each scan included errors from the background-corrected signal values for each isotope, the fractionation factor error, and an additional relative error term required to force 95% of the FC ages to be concordant. Errors for the isotopic ratios $^{207}\text{Pb}/^{235}\text{U}_c$ ($^{235}\text{U}_c = 137.88^{238}\text{U}$), $^{206}\text{Pb}/^{238}\text{U}$, and $^{207}\text{Pb}/^{206}\text{Pb}$ at each scan included errors from the background-corrected signal values for each isotope, the fractionation factor error, and an additional relative error term required to force 95% of the FC ages to be concordant. Asymmetrical negative-direction and positive-direction age errors were calculated by subtracting and adding, respectively, the isotopic ratio errors in the appropriate age equation (Chew and Donelick, 2012).

The data were considered concordant if their ratios overlapped concordia within 2σ analytical uncertainty (Spencer and others, 2016). Systematic uncertainties were propagated by quadrature prior to the calculation of the weighted mean of all magmatic samples (Horstwood and others, 2016). To determine the maximum depositional date from detrital samples, systematic uncertainties were added by quadrature to the weighted mean of the youngest cluster of grain dates overlapping within 2σ (Horstwood and others, 2016; Coutts and others, 2019).

Maximum depositional ages (MDA) defined by populations of young zircons were determined for the volcanoclastic (e.g., Tivs) and sedimentary (e.g., Ts) samples. To determine their MDAs, we calculated the youngest statistical population (youngest statistical population [YSP]; Coutts and others, 2019; Herriott and others, 2019). This approach is a reliable means of calculating an MDA with a low likelihood of yielding a date younger than the true stratigraphic age of the sampled interval (Coutts and others, 2019).

Determining the crystallization age of an igneous rock requires dating only zircons that grew immediately prior to magma crystallization (autocrystic grains; Miller and others, 2007). However, igneous rocks can contain significant quantities of antecrystic zircons (older grains that suggest long magma residence times [Hildreth, 2001; Charlier and others, 2005]) and xenocrystic grains inherited from wall rock that must be excluded prior to calculating the weighted mean (WM). Few strategies have been developed to distinguish antecrystic and xenocrystic grains in LA-ICP-MS data (e.g., Campbell and others, 2006; Seigel and others, 2018), and no standardized approach has been established. We therefore use the commonly adopted method to calculate the WM of the entire zircon distribution, noting that the resulting mean standard weighted deviation (MSWD) is much greater than 1.0, and that the probability of a zero fit indicates greater-than-expected dispersion of dates for a genetically congruent population.

ACKNOWLEDGMENTS

The authors thank GeoSep Services, LLC for their contributions to data collection. This work was funded by the U.S. Geological Survey National Cooperative Geologic Mapping Program under STATEMAP Award Number: G23AC00584-01, 2023, and the State of Alaska General Fund. The views and conclusions contained in this document are those of the authors and should not be interpreted as representing the opinions or policies of the U.S. Geological Survey. Mention of trade

names or commercial products does not constitute their endorsement by the U.S. Geological Survey or by any branch or employee of the State of Alaska.

REFERENCES

- Alaska Industrial Development and Export Authority, 2025, West Susitna Access Project: Alaska Industrial Development and Export Authority, <https://www.aidea.org/Programs/Infrastructure-Development/West-Susitna-Access>, accessed February 27, 2026.
- Black, L. Peter, Kamo, S. Lawrence, Allen, C. Michael, Davis, D. William, Aleinikoff, J. Nicholas, Valley, J. John, Mundil, Roland, Campbell, I. Hugh, Korsch, R. John, Williams, I. Stuart, and Foudoulis, Chris, 2004, Improved ²⁰⁶Pb/²³⁸U microprobe geochronology by the monitoring of trace-element-related matrix effect; SHRIMP, ID-TIMS, ELA-ICP-MS, and oxygen isotope documentation for a series of zircon standards: *Chemical Geology*, v. 205, p. 115–140, <https://doi.org/10.1016/j.chemgeo.2004.01.003>
- Bradley, Dwight, Haeussler, Peter, O'Sullivan, Paul, Friedman, Richard, Till, Alison, and Trop, Jeffrey, 2009, Detrital zircon geochronology of Cretaceous and Paleogene strata across the south-central Alaskan convergent margin: in Haeussler, P.J., and Galloway, J.P., eds., *Studies by the U.S. Geological Survey in Alaska, 2007: U.S. Geological Survey Professional Paper 1760-F*, 36 p.
- Campbell, I. Hugh, Ballard, J. Robert, Palin, J. Michael, Allen, C. Michael, and Faunes, Andrés, 2006, U-Pb zircon geochronology of granitic rocks from the Chuquicamata–El Abra porphyry copper belt of northern Chile—Excimer laser ablation ICP-MS analysis: *Economic Geology*, v. 101, no. 7, p. 1327–1344, <https://doi.org/10.2113/gsecongeo.101.7.1327>
- Chang, Zheng, Vervoort, Jeffrey D., McClelland, William C., and Knaack, Charles, 2006, U-Pb dating of zircon by LA-ICP-MS: *Geochemistry, Geophysics, Geosystems*, v. 7, no. 5, 14 p., <https://doi.org/10.1029/2005GC001100>
- Charlier, B. Laurent A., Wilson, C. John N., Lowenstern, Jacob B., Blake, Stephen, Van Calsteren, Peter W., and Davidson, Jon P., 2005, Magma generation at a large, hyperactive silicic volcano (Taupo, New Zealand) revealed by U-Th and U-Pb systematics in zircons: *Journal of Petrology*, v. 46, no. 1, p. 3–32, <https://doi.org/10.1093/petrology/egh060>
- Chew, David M., and Donelick, Richard A., 2012, Combined apatite fission-track and U-Pb dating by LA-ICP-MS and its application in apatite provenance analysis: *Mineralogical Association of Canada Short Course*, v. 42, p. 219–247.
- Coutts, David S., Matthews, W. Andrew, and Hubbard, Stephen M., 2019, Assessment of widely used methods to derive depositional ages from detrital zircon populations: *Geoscience Frontiers*, v. 10, p. 1421–1435, <https://doi.org/10.1016/j.gsf.2018.11.002>
- Donelick, Richard A., O'Sullivan, Paul B., and Ketchum, Richard A., 2005, Apatite fission-track analysis: *Reviews in Mineralogy and Geochemistry*, v. 58, p. 49–94, <https://doi.org/10.2138/rmg.2005.58.3>

- Gehrels, George E., Valencia, Victor A., and Ruiz, Joaquin, 2008, Enhanced precision, accuracy, efficiency, and spatial resolution of U-Pb ages by laser ablation–multicollector–ICP-MS: *Geochemistry, Geophysics, Geosystems*, v. 9, 13 p., <https://doi.org/10.1029/2007GC001805>
- Herriott, Thomas M., Crowley, James L., Schmitz, Mark D., Wartes, Marwan A., and Gillis, Richard J., 2019, Exploring the law of detrital zircon—LA-ICP-MS and CA-TIMS geochronology of Jurassic forearc strata, Cook Inlet, Alaska, USA: *Geology*, v. 47, no. 11, p. 1044–1048, <https://doi.org/10.1130/G46312.1>
- Hildreth, Wes, 2001, A critical overview of silicic magmatism: in *Penrose Conference on Longevity and Dynamics of Rhyolitic Magma Systems*, Mammoth, California, June 7–12, 2001, p. 6–12.
- Horstwood, Matthew S., Košler, Jan, Gehrels, George, Jackson, Simon E., McLean, Noah M., Paton, Chad, Pearson, Nicholas J., Sircombe, Keith, Sylvester, Paul, Vermeesch, Pieter, and Bowring, James F., 2016, Community-derived standards for LA-ICP-MS U-(Th-)Pb geochronology—Uncertainty propagation, age interpretation, and data reporting: *Geostandards and Geoanalytical Research*, v. 40, no. 3, p. 311–332, <https://doi.org/10.1111/ggr.12152>
- Hults, Christopher P., Wilson, Heather, Donelick, Richard A., and O’Sullivan, Paul B., 2013, Two flysch belts having distinctly different provenance suggest no stratigraphic link between the Wrangellia composite terrane and the paleo-Alaskan margin: *Lithosphere*, v. 5, p. 575–594, <https://doi.org/10.1130/L310.1>
- Miller, Joel S., Matzel, Jennifer E.P., Miller, Calvin F., Burgess, Seth D., and Miller, Robert B., 2007, Zircon growth and recycling during the assembly of large, composite arc plutons: *Journal of Volcanology and Geothermal Research*, v. 167, p. 282–299, <https://doi.org/10.1016/j.jvolgeores.2007.04.019>
- Moore, Thomas E., O’Sullivan, Paul B., Potter, Christopher J., and Donelick, Richard A., 2015, Provenance and detrital zircon geochronologic evolution of lower Brookian foreland basin deposits of the western Brooks Range, Alaska, and implications for early Brookian tectonism: *Geosphere*, v. 11, p. 93–122, <https://doi.org/10.1130/GES01043.1>
- Paces, James B., and Miller, James D., 1993, Precise U-Pb ages of Duluth Complex and related mafic intrusions, northeastern Minnesota—Geochronological insights to physical, petrogenic, paleomagnetic, and tectonomagmatic processes associated with the 1.1 Ga Midcontinent Rift System: *Journal of Geophysical Research*, v. 98, no. B8, p. 13997–14013, <https://doi.org/10.1029/93JB01227>
- Paton, Chad, Woodhead, Jon D., Hellstrom, John C., Hergt, James M., Greig, Alan, and Maas, Roland, 2010, Improved laser ablation U-Pb zircon geochronology through robust downhole fractionation correction: *Geochemistry, Geophysics, Geosystems*, v. 11, Q0AA06, <https://doi.org/10.1029/2009GC002618>
- Siegel, Coralie, Bryan, S.E., Allen, C.M., and Gust, D.A., 2018, Use and abuse of zircon-based thermometers: A critical review and a recommended approach to identify antecrystic zircons: *Earth-Science Reviews*, v. 176, p. 87–116.

- Spencer, Christopher J., Kirkland, Christopher L., and Taylor, Richard J., 2016, Strategies toward statistically robust interpretations of in situ U-Pb zircon geochronology: *Geoscience Frontiers*, v. 7, no. 4, p. 581–589, <https://doi.org/10.1016/j.gsf.2015.11.006>
- Stacey, John S., and Kramers, Jan D., 1975, Approximation of terrestrial lead isotope evolution by a two-stage model: *Earth and Planetary Science Letters*, v. 26, p. 207–221, [https://doi.org/10.1016/0012-821X\(75\)90088-6](https://doi.org/10.1016/0012-821X(75)90088-6)
- Steiger, Rolf H., and Jäger, Emil, 1977, Subcommittee on geochronology—Convention on the use of decay constants in geo- and cosmochemistry: *Earth and Planetary Science Letters*, v. 36, p. 369–371, [https://doi.org/10.1016/0012-821X\(77\)90060-7](https://doi.org/10.1016/0012-821X(77)90060-7)
- Zhang, Ming, Ewing, Rodney C., Boatner, Lynn A., Salje, Ekhard K.H., Weber, William J., Daniel, Philippe, Zhang, Yong, and Farnan, Ian, 2009, Pb* irradiation of synthetic zircon (ZrSiO₄)—Infrared spectroscopic study, reply: *American Mineralogist*, v. 94, p. 856–858, <https://doi.org/10.2138/am.2009.3167>